

Bohr's correspondence principle for atomic transport calculations

Viviana P. Ramunni and Alejandro M.F. Rivas

Conicet, Av. Rivadavia 1917, (C1033AAJ) Buenos Aires, Argentina.

(Dated: March 2, 2024)

In this work we perform a comparison between Classical Molecular Static (CMS) and quantum Density Functional Theory (DFT) calculations in order to obtain the diffusion coefficients for diluted *Fe-Cr* alloys. We show that, in accordance with Bohr's correspondence principle, as the size of the atomic cell (total number of atoms) is increased, quantum results with DFT approach to the classical ones obtained with CMS. Quantum coherence effects play a crucial role in the difference arising between CMS and DFT calculations. Also, thermal contact with the environment destroys quantum coherent effects making the classical behavior to emerge. Indeed, CMS calculations are in good agreement with available experimental data. We claim that, the atomic diffusion process in metals is a classical phenomena. Then, if reliable semi empirical potentials are available, a classical treatment of the atomic transport in metals is much convenient than DFT.

PACS numbers: 02.70.Ns, 02.70.-c, 03.65.Yz, 66.30.Fq, 66.30.J-

To characterize the crossover between the quantum and the classical worlds is a fundamental quest of modern physics. For some systems, it is clear that, classical physics arises from quantum physics in the large-number limit. This is the Bohr's correspondence principle [1].

It is not fully understood yet how the many-particle limit gives rise to classical physics, and how much of quantum physics still remains. In this framework, the environment and its temperature plays an important role for the decoherence process [2]. However, quantum coherence effects at ambient temperatures where observed in biological systems [3].

Also, for many body systems we must deal with both electrons and atomic nuclei dynamics. Due to their masses the nuclei move much slower than the electrons. Then in the Born–Oppenheimer approximation [4] the nuclei generate a static external potential in which the electrons are moving.

First principles (*Ab initio*) quantum mechanical method, such as DFT, are employed to obtain the electronic behavior. DFT reduces the quantum many-body problem to the use of functionals of the electron density [5], it is presently the most successful approach to compute the electronic structure of matter. Its applicability ranges from atoms, molecules and solids to nuclei and liquids [5]. The electron density determines the potential energy surface that represents the force field where the nuclei dynamics occurs.

In a different approach, a CMS treatment, employs phenomenological semi-empirical potentials in order to estimate this force field. Then, the quantum nature of electronic structure is not taken into account. There is a wide variety of semi-empirical potentials, which vary according to the atoms being modeled. *Ab Initio* simulations take into account the quantum nature of the electrons, which implies in a higher computational cost than CMS. Hence *ab initio* simulations are limited to smaller systems.

In this work atomic diffusion, in *Fe-Cr* diluted alloys is studied with both CMS and quantum DFT calculations, in the context of a multi-frequency model. We show that, in accordance with Bohr's correspondence principle, as the total number of atoms is increased, quantum results with DFT recover the clas-

sical ones obtained with CMS.

Quantum coherence effects, which are only taken into account by DFT, play a crucial role for both the convergence issue of the DFT results as a function of supercell size, as well as, in the difference arising between classical CMS and quantum DFT calculations.

In addition, CMS calculations are in good agreement with available experimental data for both solute and solvent diffusion coefficients. This may not be surprising for a macroscopic system especially for high temperatures that destroys any quantum coherent effect.

Diffusion plays an important role in the kinetics of many materials processes. Experimental measurements of diffusion coefficients are expensive, difficult and in some cases nearly impossible. A complimentary approach is to determine diffusivities in materials by atomistic computer simulations. In addition to predicting diffusion coefficients, computer simulations can provide insights into atomic mechanisms of diffusion processes, creating a fundamental framework for materials design strategies.

Also, *Fe-Cr* alloys at low temperatures has important technological consequences. Due to their good resistance to void swelling [6, 7], *Fe-Cr* based alloys are of special interest for nuclear applications (in Generation IV and fusion reactors).

Atomic transport theory allows to express the diffusion coefficients in terms of the atomic frequency jumps, this is commonly known as the multi-frequency model [8]. Recently, attends were made in order to describe the diffusion process by obtaining numerically the needed frequency jumps with DFT calculations. Although disagreement between the experimental and *ad-initio* based calculated diffusion coefficients were observed in bcc alloys such as *Ni-Cr* and *Ni-Fe* [9], and for α *Fe-Ni* and α *Fe-Cr* alloys [10] as well as for *Mg*, *Si* and *Cu* diluted in fcc *Al* [11]. However, in a recent work Huang et al. [12], for *Fe* based diluted alloys, have performed DFT based calculations for the tracer diffusion coefficient with a larger number of atoms (128 instead of 54 as in [10]) that are in good agreement with the experimental data.

On the other hand, one of us has recently shown [13], that tracer diffusion coefficients performed with

CMS based calculations in diluted *Ni-Al* and *Al-U* fcc alloys are in excellent agreement with available experimental data for both systems.

We focus here on the tracer self- and solute diffusion coefficients in a binary *A-S* alloy in the diluted limit. For diffusion mediated by vacancies analytical expressions, in terms of the frequency jumps, where calculated by Allnatt [14] and Le Claire [8] for fcc and bcc lattices respectively. In the 2nd-nearest-neighbor binding model, we identify the jumps as in Fig. 1. The self-diffusion coefficient can be written as,

$$D_A^* = a^2 \omega_0 C_V f_0, \quad (1)$$

where a is the lattice parameter, ω_0 is the atom-vacancy exchange frequency in pure *A* and f_0 , the self-diffusion correlation factor that is $f_0 = 0.7272$ [8] or $f_0 = 0.7814$ [14], for bcc or fcc metals respectively. At thermodynamic equilibrium the vacancy concentration depends on the temperature T as,

$$C_V = \exp \left(-\frac{E_f^V - TS_f^V}{k_B T} \right) \quad (2)$$

where k_B is the Boltzmann constant while E_f^V and S_f^V respectively denote the energy and entropy formation of the vacancy in pure *A*.

The impurity diffusion coefficient, D_S^* , depends on several jump frequencies, corresponding to the exchanges of the vacancy with the solute atom *S* and with the solvent atoms *A* near *S*, see Fig. 1.

$$D_S^* = a^2 \omega_2 f_S C_V \left(\frac{\omega_4}{\omega_3} \right), \quad (3)$$

where ω_2 is the *S*-vacancy exchange frequency and f_S is the solute correlation factor.

For bcc lattices, in the formalism of Le Claire[8], the correlation factor is

$$f_S^{bcc} = \frac{1-t}{1+t}, \quad (4)$$

where t is expressed in terms of the jump frequencies as:

$$t = \frac{-\omega_2}{\omega_2 + 3\omega_3 + 3\omega_3' + 3\omega_3'' - \frac{\omega_3\omega_4}{\omega_4 + F\omega_5} - \frac{2\omega_3'\omega_4'}{\omega_4' + 3F\omega_0} - \frac{\omega_3''\omega_4''}{\omega_4'' + 7F\omega_0}}, \quad (5)$$

with $F = 0.512$ in (5). For fcc lattices, the solute correlation factor [14] is

$$f_S^{fcc} = \left\{ \frac{2\omega_1 + 7\omega_3 F^{fcc}}{2(\omega_1 + \omega_2) + 7\omega_3 F^{fcc}} \right\}, \quad (6)$$

with F^{fcc} expressed as a function of $u = \omega_4/\omega_0$ as

$$7(1 - F^{fcc}) = \frac{u(\xi_1 u^3 + \xi_2 u^2 + \xi_3 u + \xi_4)}{\xi_5 u^4 + \xi_6 u^3 + \xi_7 u^2 + \xi_8 u + \xi_9}, \quad (7)$$

with the ξ_i coefficients calculated by Koiwa in [15].

According to the transition-state theory, in a system of N atoms, the exchange frequency between a vacancy and an atom is,

$$\omega_i = \nu_0 \exp \left(-\frac{G_m^i}{k_B T} \right) = \nu_0 \exp \left(\frac{TS_m - H_m^i}{k_B T} \right). \quad (8)$$

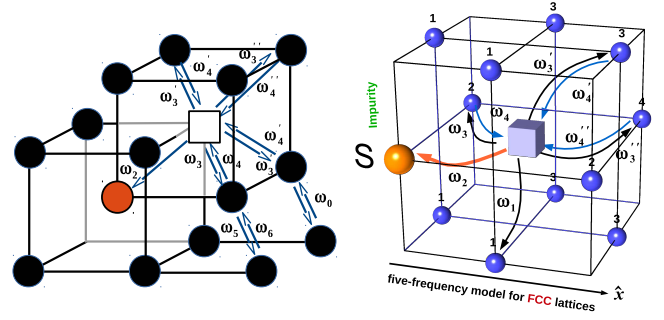


FIG. 1: (Color online) The frequencies involved in the second binding model for bcc and fcc lattices. In black/orange circles, respectively are represented the solvent and solute atoms.

In (8), G_m^i is the migration Gibbs free energy and the pre-exponential term, the "attempt frequency" ν_0 , is of the order of the Debye frequency. The Gibbs free energy is given by $G_m = H_m - TS_m$, where S_m is the migration entropy, while H_m is the enthalpy. As the volume is kept constant and the pressure is considered null, $H_m = E_m$, where E_m is the internal migration energy. Hence, following Vineyard's formulation [16], the migration frequency jumps are given by

$$\omega_i = \nu_0^* \exp(-E_m^i/k_B T). \quad (9)$$

In (9), E_m^i are the vacancy migration energies at $T = 0K$, while

$$\nu_0^* = \left(\prod_{i=1}^{3N-3} \nu_i^I \right) / \left(\prod_{i=1}^{3N-4} \nu_i^S \right) = \nu_0 \exp \left(\frac{S_m}{k_B} \right), \quad (10)$$

with ν_i^I and ν_i^S the frequencies of the normal vibrational modes at the initial and saddle points, respectively.

We present our numerical results applied to *Fe-Cr* diluted alloys. Above the melting temperature $T_{\alpha\gamma} = 1183K$, *Fe-Cr* alloys develop a paramagnetic fcc phase, while for lower temperature the structure is bcc. In this bcc phase, a magnetic transitions occurs from ferromagnetic, below the Curie temperature $T_C = 1043K$, to paramagnetic states.

In the case of the bcc phase, we performed both DFT and CMS calculations. For DFT calculations, we have employed localized basis sets as implemented in SIESTA code [17]. We have also considered spin polarization and GGA approximation in all calculations. Core electrons are replaced by nonlocal norm-conserving pseudo potentials as in Ref. [18]. Valence electrons are described by linear combinations of localized pseudoatomic orbitals. The basis sets for both elements consist in two and three localized functions for the 4s and 4p states, respectively, and five for the 3d states. The maximum cutoff radius is 5.1 Å. Calculations were carried out with 54 and 128 atom supercells, using respectively a $7 \times 7 \times 7$ and $4 \times 4 \times 4$ k-point grid, and the Methfessel-Paxton broadening scheme with a 0.3eV width. The migration barriers have been determined using SIESTA coupled to the Monomer [19].

In CMS calculations the atomic interaction are represented by EAM potentials. For the *Fe-Cr* system in

the bcc lattice we have used the potential developed by Mendeleev *et al.* [20], for the pure elements *Fe* and *Cr*, as well as, for the cross *Fe-Cr* term. While for the high temperature fcc phase, where only CMS calculations were performed, we have used the potential developed by Bonny *et al.* [21]. For all classical calculations we use a crystallite of $8 \times 8 \times 8$ with periodic boundary conditions, that is 1024 and 2048 atoms for bcc and fcc respectively. We have verified, for the bcc phase, that the results do not change if we employ a crystallite of 128 atoms. We obtain the equilibrium positions of the atoms by relaxing the structure via the conjugate gradients technique. The lattice parameters that minimize the crystal structure energy are $a_{Fe} = 2.866 \text{ \AA}$, and $a_{Fe} = 3.562 \text{ \AA}$, for bcc and fcc structures, respectively.

In Table I we show our calculations of the activation energies, formation and migration, in a perfect bcc *Fe* lattice. We show both, DTF (with 54 and 128 atoms) together with CMS calculations. Initial and saddle points configurations and their respective energies are calculated with the Monomer method [19]. We can

TABLE I: Energies and lattice parameters for the pure bcc *Fe* lattice obtained by DFT calculations with 54 and 128 atoms and by CMS calculations.

bcc - <i>Fe</i>				
	DFT ₅₄	DFT ₁₂₈	CMS	Exp.
$a(\text{\AA})$	2.885	2.885	2.866	2.866
$E_f^V(\text{eV})$	2.18	2.05	1.72	1.79 ± 0.1
$E_m^0(\text{eV})$	0.67	0.68	0.68	
$E_m^2(\text{eV})$	0.57	0.56	0.562	
$E_m^3(\text{eV})$	0.67	0.67	0.67	
$E_m^4(\text{eV})$	0.64	0.63	0.625	
$E_m^{3'}(\text{eV})$	0.63	0.60	0.558	
$E_m^{4'}(\text{eV})$	0.61	0.60	0.599	
$E_m^{3''}(\text{eV})$	0.60	0.58	0.542	
$E_m^{4''}(\text{eV})$	0.59	0.59	0.585	
$E_m^5(\text{eV})$	0.64	0.63	0.627	

observe from Table I that, as the number of atoms is increased, the energies calculated with DFT get closer to the classical ones. This effect is particularly important for the vacancy formation energy where the result obtained with CMS calculation is in accordance with the experimental result measured in [22].

For the fcc paramagnetic phase, occurring above $T_{\alpha\gamma} = 1183\text{K}$, formation and activation energies from CMS calculations in are displayed in Table II.

TABLE II: Activation energies in paramagnetic fcc *Fe-Cr* from CMS calculations, using potential of Ref.[21].

E_f^V	E_m^0	E_m^1	E_m^2	E_m^3	E_m^4	$E_m^{3'}$	$E_m^{4'}$	$E_m^{3''}$	$E_m^{4''}$
1.87	0.64	0.66	0.65	0.76	0.72	0.66	0.60	0.70	0.63

In order to compute the jump frequencies, we use expression (9), with the migration energies E_m^i reported in Tables I and II, respectively for bcc and fcc phases. For the pre-factor (10), we have taken the experimental values of the migration entropy $S_m = 2.1k_B$, as reported in [23], in all cases. While the Debye frequency has been taken as $\nu_D = 10^{13}\text{Hz}$.

For the vacancy concentration in (2), the formation entropy has been taken as $S_f^V = 4.1k_B$, from DFT calculations performed in [24], while for CMS calculations, we used $S_f^V = 2.3k_B$, as obtained in [25].

Once the jump frequencies in the multi-frequency model have been computed, the diffusion coefficients are calculated using analytical expressions (1) and (3). Also, it has been observed that, due to spontaneous magnetization [26], the self-diffusion coefficient deviates from a linear Arrhenius relationship, below the Curie temperature. This magnetization effects are, as usually, taken into account, as a correction of the activation energies Q for the ferromagnetic phase, from those in the paramagnetic Q_p (in Table I) such that,

$$Q = Q_p (1 + \alpha_X s_X^2(T)), \quad (11)$$

with $X = Fe$ or Cr and $s_X(T)$ is the ratio of the spontaneous magnetization at T to that at $T = 0\text{K}$ [27]. While $s_X(T) = 0$, in the full temperature range of the paramagnetic phase. In this respect, a direct estimation of these parameters from first principles would be of great interest. Here, as in [28], we interpolate the values of $\alpha s^2(T)$ in Ref. [27] for both, solute and solvent atoms.

In Figure 2, we show the calculated D_{Fe}^* and D_{Cr}^* , using equations (1) and (3) respectively, with the activations energies in Tables I and II for bcc and fcc phases, respectively. As we already mentioned, for the bcc phase we performed DFT, with 54 and 128 atoms, as well as, CMS calculations. Also in figure 2, experimental data taken from Refs. [26] and [28] are plotted with triangles and stars, respectively for D_{Fe}^* and D_{Cr}^* . As can be observer in Fig. 2, below

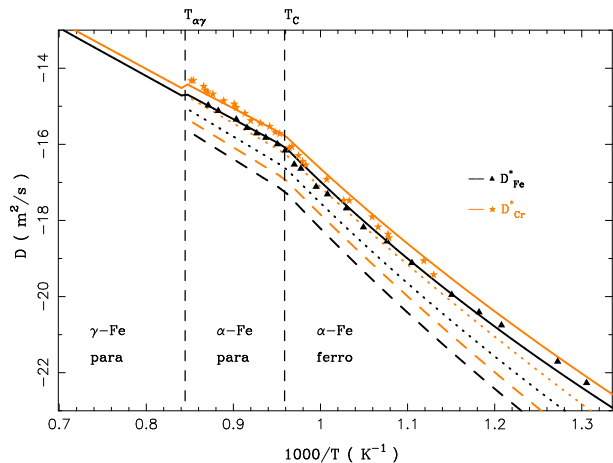


FIG. 2: (Color online) Self-diffusion (in black) and *Cr* impurity (in orange) diffusion coefficients in *Fe* from CMS and DFT calculations. Full lines correspond to CMS calculations while dotted and dashed lines for DFT with 128 and 54 atoms respectively. Experimental values for D_{Fe}^* and D_{Cr}^* , obtained from Refs. [26] and [28] are plotted with triangles and stars respectively.

the solvent melting temperature $T_{\alpha\gamma} = 1043^\circ\text{C}$, in accordance with Bohr's correspondence principle, as the size of the atomic cell (total number of atoms) is increased, quantum results with DFT approach to the classical ones obtained with CMS.

Note that the bcc supercell with 54 atoms, corresponding to a crystal of $3 \times 3 \times 3$, has a length of 8.59Å, and for 128 atoms, the $4 \times 4 \times 4$ crystal has a length of 10.14Å. In both cases, this length is lower than typical electronic quantum coherence length which are of nanometer order (4nm on Cu [29]). Then, quantum coherence effects, which are only taken into account by DFT, play a crucial role for both the convergence issue of the DFT results as a function of supercell size, as well as, in the difference arising between classical CMS and quantum DFT calculations.

Instead, with CMS, the semimpirical potential are phenomenological and the quantum coherence effects are not taken into account. Moreover, CMS calculations with 128 or 1024 atoms, give the same results.

In addition, we must not expect to observe quantum effects for such macroscopic systems especially at the high temperatures here described. In that case, the interaction of the system with the thermal environment implies in decoherence effects, where the classical limit is expected to be recovered [2].

Indeed, our results obtained with CMS calculations are in good agreement with available experimental data for both, tracer solute and solvent diffusion coefficients. Note that, similar results have been obtained using, the also classical method, Kinetic Monte Carlo algorithm with temperature dependent pair interactions [30].

It must be emphasized that the agreement between CMS based calculations and experimentally measured diffusion coefficients is not fortuitous, it has been recently observed for diffusion in *Al-U* and *Ni-Al* fcc lattices [13]. While for this former DFT calculation underestimated the diffusion coefficients [31].

Several possible explanations of the fact that DFT calculation are not in agreement with experiments for the diffusion coefficients where argued in [9]. We claim

here that this is due to quantum coherence effects arising from DFT calculations for the size of the simulation cell being small. As the size of the simulation cell is increased the DFT results converge to the experimental values that can be obtained with CMS calculations which is much less expensive.

For the fcc phase, where diffusion coefficients have not yet been measured, our CMS calculations predicts the diffusion behavior.

In summary, in this work we have performed a comparison between quantum DFT and CMS calculations in order to obtain the diffusion properties in bcc *Fe-Cr* diluted alloys. In accordance with Bohr's correspondence principle, as the total number of atoms is increased, the diffusion coefficients obtained with quantum DFT calculations, approach the classical ones obtained with CMS. For DFT calculations, the electronic quantum coherence plays a crucial role that is related with the size of the simulation cell. Also, thermal contact with the environment as the effect of killing coherence effects making the classical behavior to emerge. Indeed, results obtained with CMS calculations are in good agreement with available experimental data for both solute and solvent diffusion coefficients.

Hence, the atomic diffusion process in metals is a classical phenomena, for which the large number of atoms and the temperature has suppressed any quantum coherent effect. Then, if reliable semi empirical potentials are available, a classical treatment of the atomic transport in metals is much convenient than DFT.

The comparison between DFT and CMS calculation is then purposed as a tool to investigate the effective size of quantum effects, such as coherence length.

Acknowledgements

This work was partially financed by CONICET PIP-00965/2010.

-
- [1] N. Bohr, eds. L. Rosenfeld, J. Nielsen, J. Rud, , *Niels Bohr, Collected Works*, **3**, North-Holland, (1976).
 - [2] W. H. Zurek, *Phys. Today* **44** (10), 36 (1991).
 - [3] E. Collini, et al. *Nature* **463**, 644-647 (2010).
 - [4] M. Born and J. R. Oppenheimer, *Annalen der Physik* (in German) **389** (20), 457 (1927).
 - [5] W. Kohn, *Rev. Mod. Phys.* **71**, 1253 (1998).
 - [6] R. Klueh and A. Nelson, *J. Nucl. Mat.* **371**, 37 (2007).
 - [7] S. J. Zinkle and J. T. Busby, *Mater. Today* **12**, 12 (2009).
 - [8] A.D. Le Claire, ed. Eyring, *Physical chemistry: an advanced treatise*, Vol. 10. Academic Press (1970).
 - [9] J.D. Tucker, et. al, *J. of Nucl. Mat.* **405**, 216 (2010).
 - [10] S. Choudhury, et. al, *J. of Nucl. Mat.* **411**, 1 (2011).
 - [11] M. Mantina, et. al, *Acta Materialia* **57** 4102 (2009).
 - [12] S. Huang, et. al, *Acta Materialia* **58**, 1982 (2010).
 - [13] V.P. Ramunni, *Comm. Mat. Science.* **93**, 112 (2014).
 - [14] A.R. Allnat, *J. Phys. C: Sol. State Phys.* **14**, 5453-5466 (1981), *ibid* 5467-5477 (1981).
 - [15] M. Koiwa and S. Ishioka, *Phil. Mag.* **A47**, 927 (1983).
 - [16] G.H. Vineyard, *J. Phys. Chem. Solids*, **3**, 121 (1957).
 - [17] J. M. Soler, et.al, *J. Phys.: Cond. Mat.* **14**, 2745 (2002).
 - [18] E. Martínez, et. al , *Phys. Rev. B* **86**, 224109 (2012).
 - [19] V.P. Ramunni, M.A. Alurralde and R.C. Pasianot, *Phys. Rev. B* **74**, 054113 (2006).
 - [20] M.I. Mendelev, et. al, *Phil. Mag.* **83**, 3977 (2003).
 - [21] G. Bonny, N. Castin and D. Terentyev, *Model. Simul. Mater. Sci. Eng.* **21**, 085004 (2013).
 - [22] L. De Schepper et. al. *Phy. Rev. B* **27**, 5257(1983).
 - [23] H. Mehrer, N. Stolica, and N. A. Stolwijk, Ed. H. Mehrer *Diffusion in Solid Metals and Alloys*, Vol. 26 (Springer, Berlin, 1990).
 - [24] G. Lucas and R. Schaublin, *Nucl. Instr. Methods Phys. Res., Sect. B* **267**, 3009 (2009).
 - [25] M.I. Mendelev and Y. Mishin, *Phys. Rev. B* **80**, 144111 (2009).
 - [26] Y. Iijima, K. Kimura, K. Hirano, *Acta Metallurgica*, **36**, 10, 2811-2820 (1988).
 - [27] J. Crangle, G.M. Goodman, *Proc. R. Soc. London Ser. A* **321**, 477 (1971). H. H. Potter, *ibid* **146**, 362 (1934).
 - [28] C.G. Lee, et. al , *Mater. Trans., JIM* **31**, 255 (1990).
 - [29] P. Wahl, et. al, *Phys. Rev. Lett.* **91**, 106802 (2003).
 - [30] O. Senninger, et. al, *Acta Materialia* **73**, 97 (2014).
 - [31] C.L. Zacherl, PhD thesis, Penn State University (2012).